Plasma Proteomics in Morquio-A Disease

Subjects: Biochemistry & Molecular Biology

Contributor: María L. Couce

Mucopolysaccharidosis type IVA (MPS IVA) is a lysosomal disease caused by mutations in the gene encoding the enzymeN-acetylgalactosamine-6-sulfate sulfatase (GALNS), and is characterized by systemic skeletal dysplasia due to excessive storage of keratan sulfate (KS) and chondroitin-6-sulfate in chondrocytes. Although improvements in the activity of daily living and endurance tests have been achieved with enzyme replacement therapy (ERT) with recombinant human GALNS, recovery of bone lesions and bone growth in MPS IVA has not been demonstrated to date. Moreover, no correlation has been described between therapeutic efficacy and urine levels of KS, which accumulates in MPS IVA patients.

biomarkers enzyme replacement therapy lysosomal disorders proteomics

1. Introduction

Mucopolysaccharidosis type IVA (MPS IVA, OMIM #253000) or Morquio A syndrome is an autosomal recessive disease caused by mutations in the *GALNS* gene. This molecular defect results in a deficiency in the enzyme N-acetylgalactosamine-6-sulfate sulfatase (GALNS, E.C.3.1.6.4) [1][2][3], which degrades the specific glycosaminoglycans(GAGs) keratan sulfate (KS) and chondroitin-6-sulfate (C6S) [4][5][6][7]. These GAGs accumulate in multiple tissues, mainly bone, cartilage, heart valves, and cornea, leading to progressive systemic skeletal dysplasia [8][9]. Significant non-skeletal manifestations, including respiratory disease, spinal cord compression, cardiac disease, impaired vision, hearing loss, and dental problems, have also been described in MPS IVA patients [10][11][12][13]. MPS IVA is more frequently associated with severe and extensive skeletal manifestations than the other MPS types. Specifically, hypermobility of the joints is a characteristic of MPS IVA that distinguishes this disease from other forms of MPS. Furthermore, cognitive involvement is generally absent in MPS IVA [14]. Among untreated patients, respiratory failure is the primary cause of death, which typically occurs during the second or third decades of life [15][16].

Currently, two therapies for MPS IVA are used in clinical practice: enzyme replacement therapy (ERT) with recombinant human GALNS; and hematopoietic stem cell transplantation (HSCT) [5][11]. ERT and HSCT are based on the cross-correction principle, where by lysosomal enzymes are taken up by the cells of deficient recipients and targeted to the lysosomes via the mannose-6-phosphate receptor. However, as described for other lysosomal storage diseases, ERT for MPS IVA suffers from several limitations, including the need for weekly infusions of 4–6 h; rapid clearance due to a short half-life (35 min in human, 2 min in mouse) [17][18][19]; a high price [19][20]; limited penetration of the avascular cartilage; and immunological responses against the infused enzyme [16][17][21]. Moreover, clinical trials have shown little improvements in terms of bone growth and skeletal dysplasia. There is no

definitive therapy that markedly improves bone and cartilage lesions in MPS IVA [14][18][19][20]. Potential biomarkers proposed in recent studies include KS, C6S, and blood levels of collagen II [22][23]. Although clinical trials have studied urinary KS as a potential biomarker, it has not been demonstrated that decreases in this parameter correlate with clinical improvement. Urinary KS originates in the kidneys but does not reflect the involvement of bone or other relevant tissues in MPS IVA, and is considered a pharmacokinetic marker but not a surrogate biomarker. The identification of valid biomarkers of bone lesions to evaluate therapeutic efficacy thus remains an unmet need. While bone cartilage samples are the best samples in which to search for candidate biomarkers of MPS IVA, the objective of this study was to assess the validity of candidate plasma biomarkers proposed in previous studies and to search for new biomarkers. To this end, we carried out both quantitative and qualitative proteomic analyses of plasma samples from.

Within rare disease research, proteomics is a fast-growing field. Approaches based on liquid chromatography-tandem mass spectrometry (LC-MS/MS), which are used to search for biomarkers in other human diseases [24][25][26][27][28], are key tools used to study normal and affected tissues and body fluids (e.g., plasma) in rare diseases [29].

Disease states involve alterations in the expression levels, phosphorylation states, and post-transcriptional modifications of proteins. Therefore, proteomics techniques have been applied to the study of normal and pathological conditions to search for biological information that could further our understanding of pathophysiological mechanisms and identify novel disease biomarkers [26][28][30]. Specific disease biomarkers identified using proteomics techniques could help improve diagnostic and prognostic precision and serve as key tools for the evaluation of treatment outcomes [24][25][26][27][28][29][30][31].

2. Qualitative Analysis of Proteins in Plasma Samples

In this study, we identified all proteins in plasma samples using data-dependent acquisition (DDA)-LC-MS/MS. Subsequent analysis was limited to proteins identified with 1% error (i.e., those with a false discovery rate (FDR) < 1). To obtain the most representative proteins per group, we selected proteins identified in at least n-1 samples per group (where n is the number of samples per group). The Venn diagram in **Figure 1** depicts the distribution of proteins in each of the 4 groups, and indicates those that were common to multiple groups.

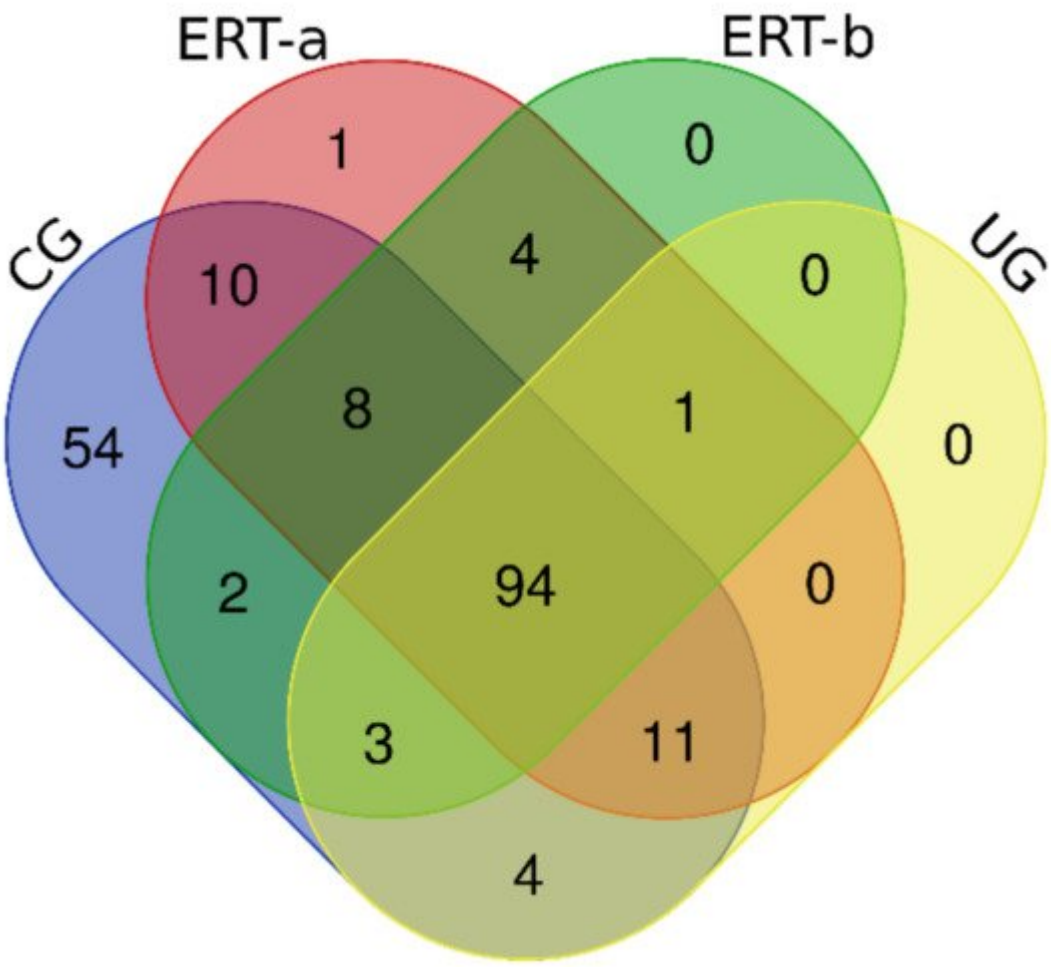

Figure 1. Venn diagram showing the distribution of proteins identified in the qualitative proteomic analysis across each of the 4 study groups.

Once we determined the proteins characteristic of each group, we performed a functional analysis using the FunRich program. This analysis allows us to characterize the behavior of the proteins identified in each group. Comparison of ERT-a and ERT-b samples revealed a favorable evolution (i.e., values obtained in ERT-a or ERT-b were close to thoseobtained for control samples) for certain proteins. Next, we selected groups of proteins in which alterations are observed in MPS IVA, and analyzed their behavior in each study group. From these, we identified proteins involved in hemostasis, bone regeneration, reorganization of theextracellular matrix and collagen, the immune response, complement system, and oxidative stress.

Among proteins implicated in hemostasis (blood coagulation, fibrin clot formation, and blood coagulation intrinsic pathway), we observed that values obtained for ERT-a samples (i.e., those collected 6 days after the preceding enzyme infusion) were closer to those of control samples than to ERT-b samples (**Figure 2**a). This result suggests that blood levels of these proteins require several days to stabilize after ERT infusion. A similar effect was observed for proteins implicated in different aspects of hemostatic processes, including platelet activation, platelet aggregation, and platelet degranulation (**Figure 2**b).

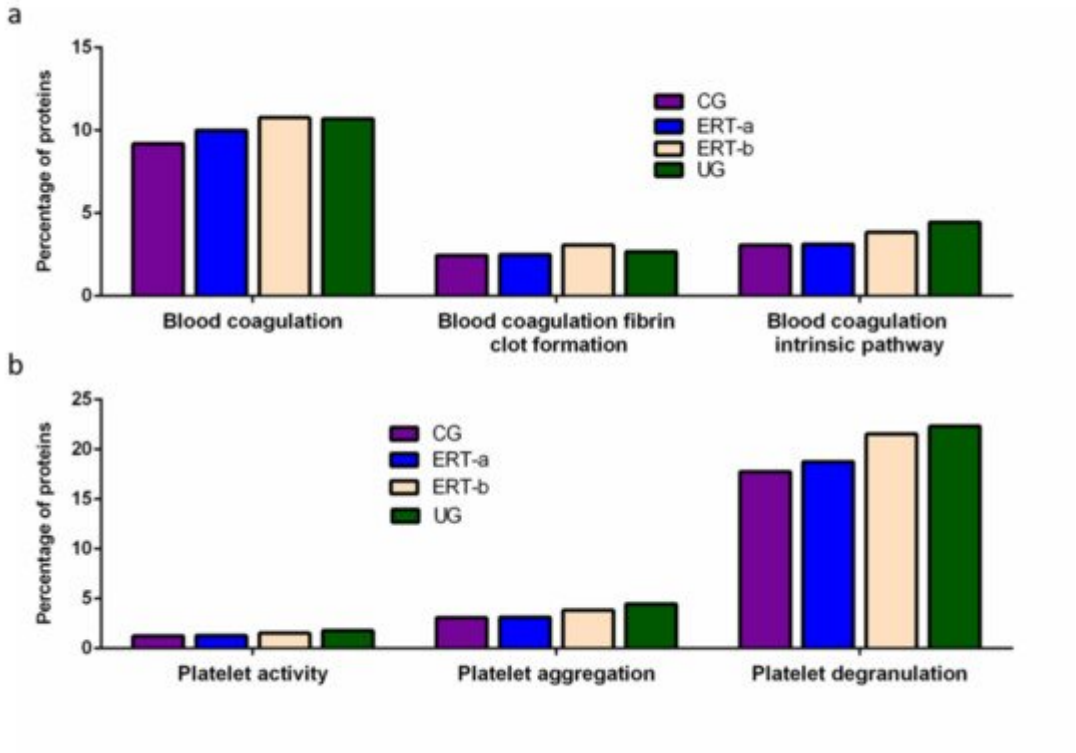

Figure 2. Functional enrichment analysis using FunRich. Proteins identified in each the different groupswere submitted to molecular functional analysis according to their involvement inhemostasis (**a**) and platelet function (**b**). CG, control group; ERT-a, patients sampled before ERT; ERT-b, patients sampled 24 h after ERT; UG, untreated group.

Other proteins identified in the proteomic analysis were implicated in bone regeneration and collagen function. Analysis of the behavior of these proteins showed that ERT had a negative regulatory effect on some (including proteins involved in mineralization, ossification, and osteoblast differentiation) and a positive regulatory effect on others (bone resorption and regulation of bone mineralization) (**Figure 3**a). In the case of proteins that were negatively regulated, ERT required more than 24 h to affect protein expression. Conversely, in the case of positively regulated proteins (involved in bone resorption and osteoblast differentiation) plasma levels increased after treatment in the ERT-b group (**Figure 3**a).

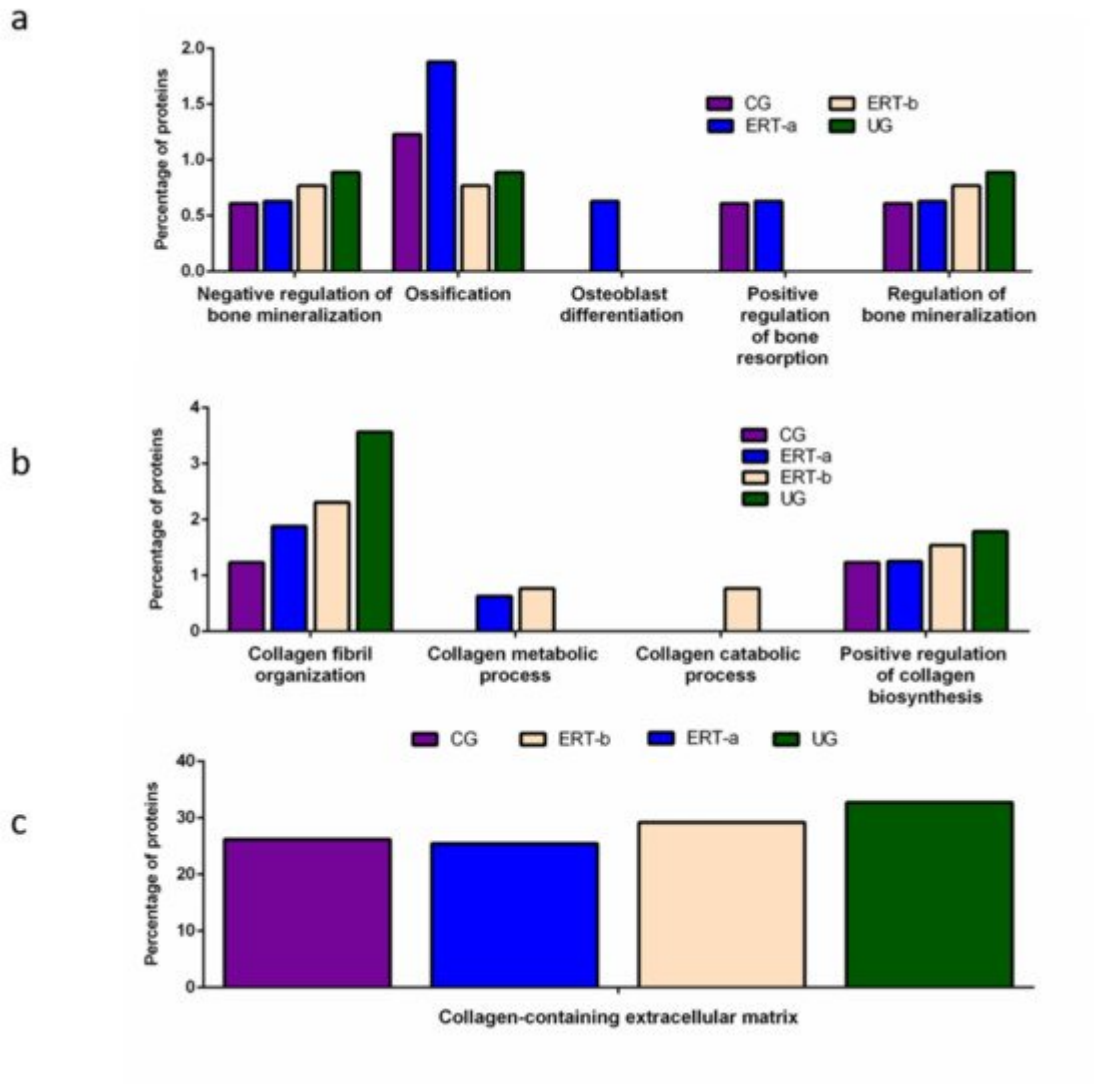

Figure 3. Functional enrichment analysis using FunRich. Proteins identified in each the different groups were submitted to molecular functional analysis according to their involvement in: (**a**) processes that occur at the bone level; (**b**) collagen function (activity/processing/biosynthesis); (**c**) collagen-containing extracellular matrix. CG, control group; ERT-a, patients sampled before ERT; ERT-b, patients sampled 24 h after ERT; UG, untreated group.

Proteomic analysis of proteins involved in collagen function revealed values close to those of the control group for proteins related to a positive regulation of the collagen biosynthesis (**Figure 4**b) in the ERT-a group. Moreover, in the ERT-a study group, we observed decreases in the expression of proteins implicated in collagen biosynthesis and collagen fibril organization. The behavior of proteins involved in metabolic and catabolic processes was unaltered after ERT administration (data not shown).

A search for proteins that interact with collagen in the extracellular matrix identified 5 proteins; P02671, P02751 (fibronectin 1), P02675, P51884 (lumican), and P02679.

We detected a relatively high number of proteins involved in the immune response. The results of the functional analysis of these proteins are shown in **Figure 4** and **Figure 5**. **Figure 4**a shows the results of functional

enrichment analysis of proteins implicated in inflammation, including proteins related to interleukins (ILs) IL-1, IL-1β, IL-6, IL-8, and to interferon γ (TNF-γ). Proteins were grouped according to their participation in different processes, including the cellular response to interferon γ, the cellular response to IL-1, the cellular response to IL-6, positive regulation of IL-1 secretion, positive regulation of IL-1β secretion, negative regulation of IL-1β secretion, negative regulation of IL-6 production, and positive regulation of IL-8 biosynthesis. In all cases, we observed a reduction in the expression of the proteins of interest24 h after ERT administration (ERT-b), except for proteins involved in positive regulation of IL-1 secretion (no change observed after ERT). In UG we detected 1.79% of proteins related to IL-1, IL-1β, and TNF-γ. This corresponding value in the ERT-a group (1.25%) was closer to that observed in controls (1.23%). In the case of proteins related to IL-6 and IL-8 we detected values of 0.88% in UG,0.63% in ERT-a, and 0.61 in the control group.

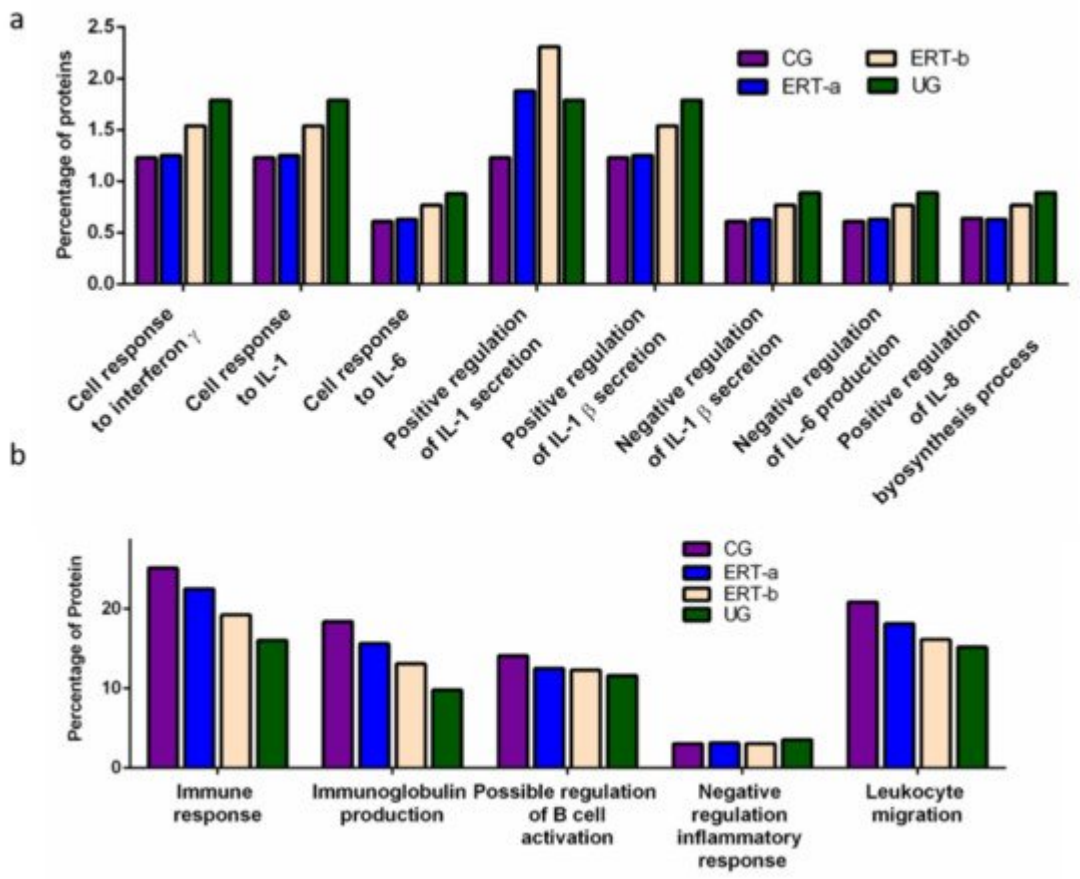

Figure 4. Functional enrichment analysis using FunRich. Proteins identified in each the different groups were submitted to molecular functional analysis according to their involvement in the immune response: proteinsrelated tointerleukins (ILs) IL-1, IL-1β, IL-6, IL-8, and interferon γ (**a**); proteins involved in immunoglobulin production, positive regulation of B-cell activation, negative regulation of the inflammatory response, and leukocyte migration (**b**).

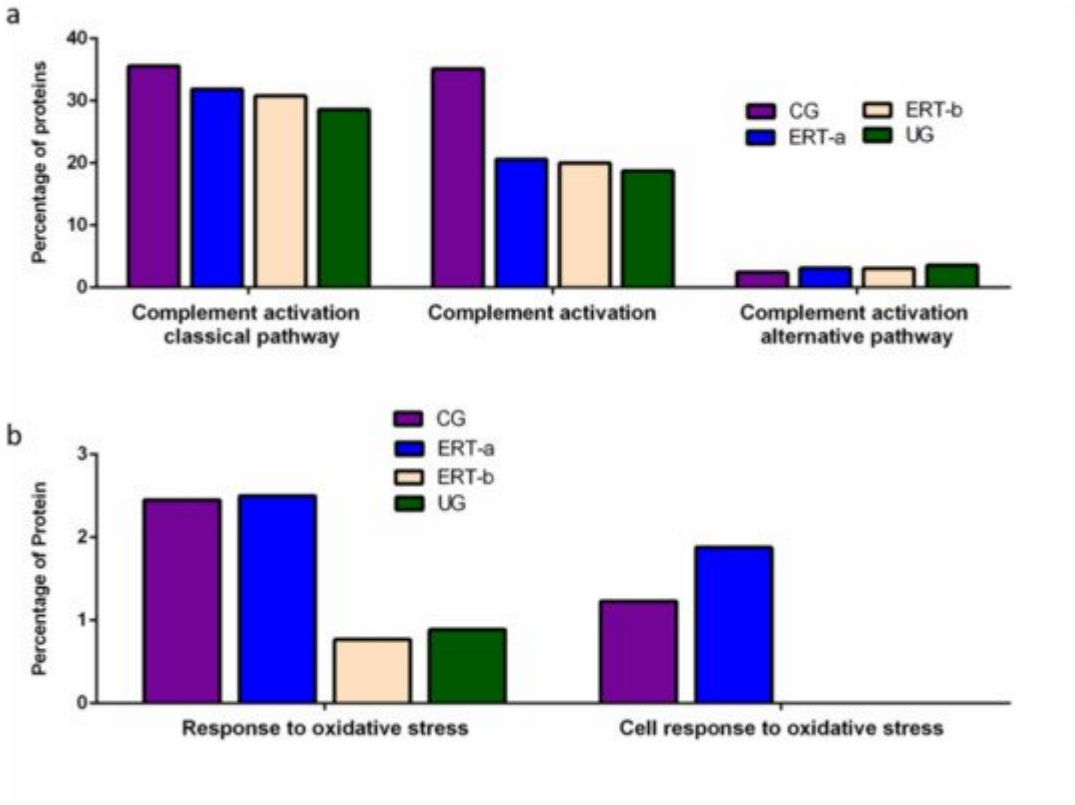

Figure 5. Functional enrichment analysis using FunRich. Proteins identified in each of the different groups were submitted to molecular functional analysis according to their involvement in immune processes: proteins involved in the classical or alternative complement activation pathways (**a**); proteins involved in the response to oxidative stress (**b**).

The results of the functional enrichment analysis of proteins involved in biological processes related tothe immune response, immunoglobulin production, positive regulation of B cell activation, negative regulation inflammatory response, and leukocyte migrationare shown in **Figure 4**b. In all cases, ERT increased the expression of proteins involved in each of these biological processes, except for negative regulation of the inflammatory response.

Functional enrichment analysis was also performed to identify protein partner expression between groups of proteins related to inflammatory processes (biological processes relating to (i) the complement system, including the classical complement activation pathway, (ii) general complement activation, and (iii) the alternative complement activation pathway). The results (**Figure 5**) reveal a positive effect of ERT, although levels of protein expression levels did not reach those observed in the control group (**Figure 5**a). **Figure 5**b shows the results of the functional enrichment analysis of proteins involved in the oxidative stress response. Treatment (ERT-a) resulted in protein levels similar to those observed in the control group for proteins involved in both complement activation and oxidative stress.

3. SWATH Quantitative Analysisof Proteins in Plasma Samples

Quantitative analysis of proteins using SWATH revealed significant alterations in the expression of multiple proteins in the ERT-a and ERT-b groups relative to the control group (**Table 1**).

Table 1. Changes in plasma protein expression detected by SWATH in any of the patient groups (UG, ERT-a, or ERT-b) relative to the control group.

Group Comparison	Proteins with Altered Expression*	Upregulated Proteins	Downregulated Proteins
UG vs CG	14	12	2
ERT-a vs CG	8	5(2 only in ERT-a)	1
ERT-b vs CG	14	10(2 only in ERT-b)	1

Quantitative Analysis Using SWATH

Proteins that were upregulated or down regulated in each group may be relevant in MPS IVA disease. Differences in protein expression in the UG may reveal candidate biomarkers of disease. Proteins upregulated or downregulated in the ERT-a and ERT-b groups can be considered as markers of disease evolution as they were altered before treatment. We identified certain proteins that were downregulated by more than 100 fold, including AMBP, ASM3B, KV117, and ZBTB4 (highlighted in dark red in **Figure 6** and **Table 2**).

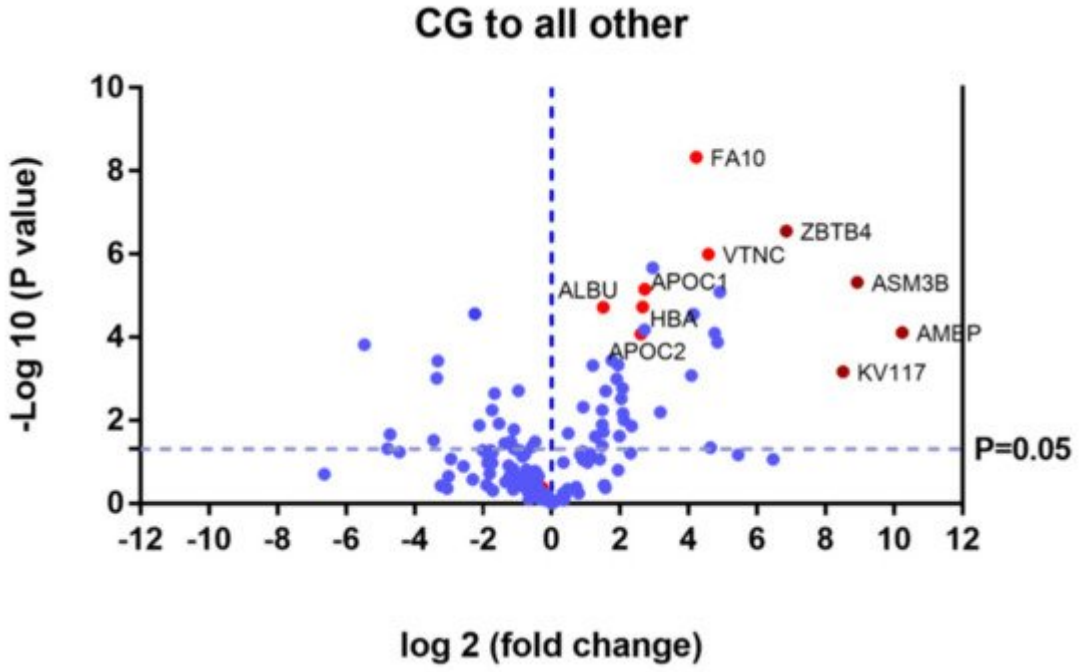

Figure 6. Volcano plot showing the results of the SWATH analysis of plasma protein expression. Data are represented as the results obtained for the control group relative to all other groups (UG, ERT-a, and ERT-b). Graph shows the negative base 10 log of the *p*-value plotted against the base 2 log of the fold change for each

protein included in the SWATH analysis. Changes were considered significant at $p < 0.05$ and fold change >1.5 compared with control group.

Table 2. Changes in plasma protein expression detected in all patient groups (UG, ERT-a, and ERT-b) relative to the control group. Protein expression is considered altered in cases in which $p < 0.05$ and the fold change >1.5 (upregulated proteins) or <0.6 (downregulated proteins).

Uniprot Code	Protein Code	Protein Name	*p*-Value	Fold Change
Downregulated in UG, ERT-a, and ERT-b				
P01860	IGHG3	Immunoglobulin heavy constant gamma 3	3.30×10^{-5}	Only CG
P02741	CRP	C-reactive protein	8.93×10^{-3}	Only CG
P02760	AMBP	Protein AMBP	7.75×10^{-5}	0.0008
Q92485	ASM3B	Acid sphingomyelinase-like phosphodiesterase 3b	4.80×10^{-6}	0.0021
P01599	KV117	Immunoglobulin kappa variable 1–17	6.69×10^{-4}	0.0027
Q9P1Z0	ZBTB4	Zinc finger and BTB domain-containing protein 4	2.81×10^{-7}	0.0086
P01780	HV307	Immunoglobulin heavy variable 3–7	8.23×10^{-6}	0.0333
P22352	GPX3	Glutathione peroxidase 3	1.31×10^{-4}	0.0349
P35542	SAA4	Serum amyloid A-4 protein	8.01×10^{-5}	0.0368
P01766	HV313	Immunoglobulin heavy variable 3–13	4.50×10^{-2}	0.0402
P04004	VTNC	Vitronectin	1.00×10^{-6}	0.0417
P00742	FA10	Coagulation factor X	4.71×10^{-9}	0.0535
P02042	HBD	Hemoglobin subunit delta	2.79×10^{-5}	0.0565

Uniprot Code	Protein Code	Protein Name	*p*-Value	Fold Change
A0A075B6J9	LV218	Immunoglobulin lambda variable 2–18	8.30×10^{-4}	0.0588
P02753	RET4	Retinol-binding protein 4	6.31×10^{-3}	0.1103
P06312	KV401	Immunoglobulin kappa variable 4–1	2.12×10^{-6}	0.1292
P02654	APOC1	Apolipoprotein C-I	7.01×10^{-6}	0.1515
P02765	FETUA	Alpha-2-HS-glycoprotein	6.60×10^{-5}	0.1527
P69905	HBA	Hemoglobin subunit alpha	1.86×10^{-5}	0.1585
P02655	APOC2	Apolipoprotein C-II	8.27×10^{-5}	0.1642
P00915	CAH1	Carbonicanhydrase 1	1.37×10^{-2}	0.1984
P02751	FINC	Fibronectin	9.79×10^{-3}	0.2304
A0A0B4J1Y8	LV949	Immunoglobulin lambda variable 9–49	6.70×10^{-3}	0.2353
P02746	C1QB	Complement C1q subcomponent subunit B	1.68×10^{-3}	0.2381
P00738	HPT	Haptoglobin	3.00×10^{-3}	0.2445
P01857	IGHG1	Immunoglobulin heavy constant gamma 1	2.37×10^{-2}	0.2519
P01834	IGKC	Immunoglobulin kappa constant	4.67×10^{-4}	0.2591
P68871	HBB	Hemoglobin subunit beta	1.01×10^{-3}	0.2681
P01859	IGHG2	Immunoglobulin heavy constant gamma 2	3.60×10^{-4}	0.2959

Uniprot Code	Protein Code	Protein Name	*p*-Value	Fold Change
P29622	KAIN	Kallistatin	1.99×10^{-3}	0.3344
P02743	SAMP	Serum amyloid P-component	1.91×10^{-2}	0.3509
P02768	ALBU	Serum albumin	1.92×10^{-5}	0.3509
P02787	TRFE	Serotransferrin	4.11×10^{-2}	0.3571
P02749	APOH	Beta-2-glycoprotein 1	1.26×10^{-2}	0.3584
P02679	FIBG	Fibrinogen gamma chain	5.71×10^{-3}	0.3597
P02763	A1AG1	Alpha-1-acid glycoprotein 1	2.43×10^{-2}	0.4115
P05543	THBG	Thyroxine-binding globulin	4.82×10^{-4}	0.4348
		Upregulated in UG, ERT-a, and ERT-b		
P01619	KV320	Immunoglobulin kappa variable 3–20	0.0005	Not found CG
P80748	LV321	Immunoglobulin lambda variable 3-21	0.0179	Not found CG
B9A064	IGLL5	Immunoglobulin lambda-like polypeptide 5	0.0002	44.0529
P01615	KVD28	Immunoglobulin kappa variable 2D–28	0.0474	27.4725
P0DOY2	IGLC2	Immunoglobulin lambda constant 2	0.0217	26.1780
P35858	ALS	Insulin-like growth factor-binding protein complex acid labile subunit	0.0299	10.8460
P10909	CLUS	Clusterin	0.0010	10.1523
P02750	A2GL	Leucine-rich alpha-2-glycoprotein	0.0004	9.9800
P01023	A2MG	Alpha-2-macroglobulin	0.0000	4.7170
P00734	THRB	Prothrombin	0.0132	4.3178

Of the proteins that were the upregulated and downregulated in the UG, ERT-a, and ERT-b groups relative to controls, 31% were related to immune system function. It is important to point out that most of the proteins for which changes in expression were observed in the study groups were down regulated. In addition to upregulated

Uniprot Code	Protein Code	Protein Name	*p*-Value	Fold Change
P06396	GELS	Gelsolin	0.0057	3.3223
P19823	ITIH2	Inter-alpha-trypsin inhibitor heavy chain H2	0.0023	3.1536
Q96IY4	CBPB2	Carboxypeptidase B2	0.0121	2.8977
Q08380	LG3BP	Galectin-3-binding protein	0.0361	2.5880
P08185	CBG	Corticosteroid-binding globulin	0.0325	2.2763
A0A0A0MS15	HV349	Immunoglobulin heavy variable 3–49	0.0482	2.1418
A0A0C4DH38	HV551	Immunoglobulin heavy variable 5–51	0.0165	2.1345

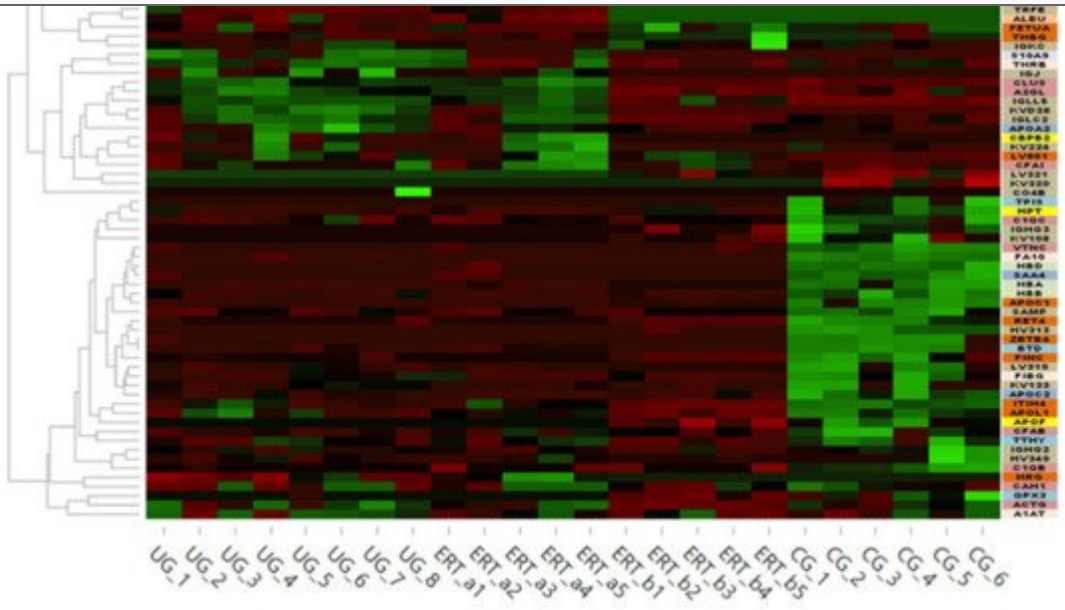

Figure 7. Heatmap depicting the expression profiles of different proteins (also shown in **Table 2**, **Table 3** and **Table 4**) as determined by SWATH quantitative analysis. The relative abundance of each protein is reflected by the colors in the heatmap, based on the z-score of the protein's normalized peak area. The dendrogram represents the biological replicates of the UG, ERT-a, ERT-b, and CG groups. Proteins, listed in the sidebar on the right, are color coded according to their function, as follows: apolipoprotein-related proteins, dark green; blood coagulation, purple; calcium binding, dark orange; carrier proteins, light green; cytoskeletal proteins, light pink; immune system, grey; metabolic processes, yellow; metabolic interconversion, light blue; other functions, white; protein binding, pink; transport, light grey.

Table 3. Changes in protein expression in the untreated group relative to all other groups. Protein expression is considered altered in cases in which $p < 0.05$ and the fold change >1.5 (upregulated proteins) or <0.6 (downregulated proteins).

Uniprot Code	Protein Code	Protein Name	*p*-Value	Fold Change
Upregulated in Untreated Group				

Uniprot Code	Protein Code	Protein Name	*p*-Value	Fold Change
P06702	S10A9	Protein S100-A9	0.0036	17.4468
P01615	KVD28	Immunoglobulin kappa variable 2D-28	0.0008	5.6619
P80748	LV321	Immunoglobulin lambda variable 3-21	0.0007	4.6098
P01594	KV133	Immunoglobulin kappa variable 1-33	0.0182	3.5490
P02652	APOA2	Apolipoprotein A-II	0.0197	2.8151
P01591	IGJ	Immunoglobulin J chain	0.0395	2.4479
P63261	ACTG	Actin, cytoplasmic 2	0.0304	2.2374
P00734	THRB	Prothrombin	0.0265	2.0770
B9A064	IGLL5	Immunoglobulin lambda-like polypeptide 5	0.0420	1.9341
P01714	LV319	Immunoglobulin lambda variable 3-19	0.0313	1.7496
P01009	A1AT	Alpha-1-antitrypsin	0.0014	1.6875
P02747	C1QC	Complement C1q subcomponent subunit C	0.0223	1.6522
		Downregulated in Untreated Group		
P02746	C1QB	Complement C1q subcomponent subunit B	0.0329	0.1549
P08697	A2AP	Alpha-2-antiplasmin	0.0275	0.4938

Table 4. Changes in protein expression in the ERT-a or ERT-b groups relative to all other groups. Protein expression is considered altered in cases in which $p < 0.05$ and the fold change >1.5 (upregulated proteins) or <0.6 (downregulated proteins).

Uniprot Code	Protein Code	Protein Name	*p*-Value	Fold Change
		Upregulated in ERT-a		
P0DJI8	SAA1	Serum amyloid A-1 protein	0.0487	Only ERT-a
Q13790	APOF	Apolipoprotein F	0.0487	Only ERT-a
A0A0C4DH68	KV224	Immunoglobulin kappa variable 2-24	0.0109	6.1248
P05156	CFAI	Complement factor I	0.0065	5.2409
A0A075B6I0	LV861	Immunoglobulin lambda variable 8-61	0.0386	3.1547
P43251	BTD	Biotinidase	0.0301	2.8996

P04196	HRG	Histidine-rich glycoprotein	0.0224	1.5688
Downregulated in ERT-a				
P02747	C1QC	Complement C1q subcomponent subunit C	0.0465	0.5069
Uniprot Code	**Protein Code**	**Protein Name**	***p*-Value**	**Fold Change**
Upregulated in ERT-b				
P60174	TPIS	Triosephosphateisomerase	0.0487	Only ERT-b
O00391	QSOX1	Sulfhydryl oxidase 1	0.0487	Only ERT-b
A0A0C4DH67	KV108	Immunoglobulin kappa variable 1-8	0.0028	Only ERT-b
P0C0L5	CO4B	Complement C4-B	0.0029	17.9592
O14791	APOL1	Apolipoprotein L1	0.0480	2.2700
P20742	PZP	Pregnancyzone protein	0.0418	2.1171
P06396	GELS	Gelsolin	0.0080	2.0649
P00751	CFAB	Complement factor B	0.0184	2.0058
P19823	ITIH2	Inter-alpha-trypsin inhibitor heavy chain H2	0.0093	1.9167
P01023	A2MG	Alpha-2-macroglobulin	0.0093	1.8574
P08697	A2AP	Alpha-2-antiplasmin	0.0298	1.8165
Q14624	ITIH4	Inter-alpha-trypsin inhibitor heavy chain H4	0.0389	1.7428
P05546	HEP2	Heparin cofactor 2	0.0421	1.6111
Downregulated in ERT-b				
P02766	TTHY	Transthyretin	0.0224	0.2358

In order to shown the results in a better way, we represent a heatmap using the proteins up and down regulated shown in **Table 2**. Moreover, the proteins were classified into different functions and were highline in different colors. Among these proteins, those shown in **Figure 8** and **Figure 9** stand out.

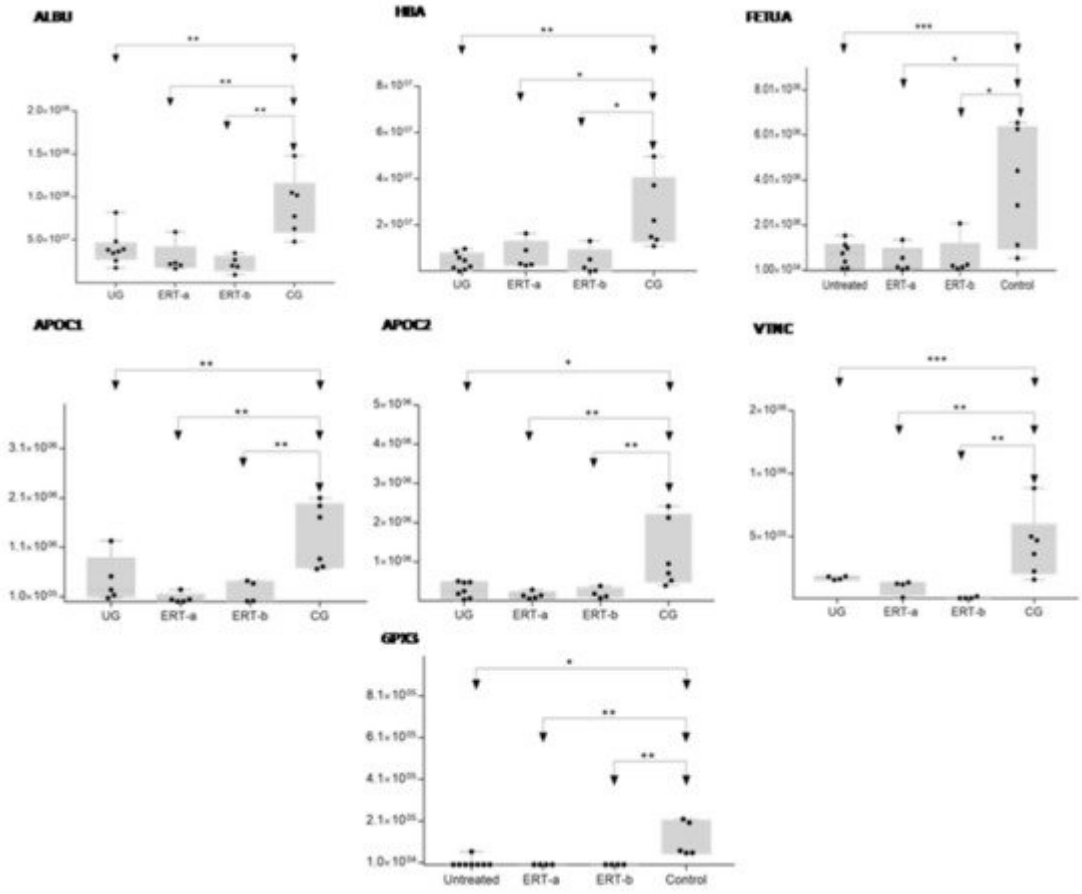

Figure 8. Box plot depicting expression levels of the6 most relevant plasma proteins (ALBU, HBA, FETUA, APOC1, APOC2, VTNC, and GPX3) for which downregulation was observed in the UG and ERT-a and ERT-b groups relative to the control group (CG). Each data point represents the median protein expression value obtained in an individual sample. The line inside the box represents the median of all values obtained. The upper and lower limits of the box represent the first and third quartiles. Whiskers represent the minimum and maximum values within 1.5 times the interquartile range. Any data points not included between the whiskers are considered outliers. * $p < 0.05$; ** $p < 0.01$; *** $p < 0.001$.

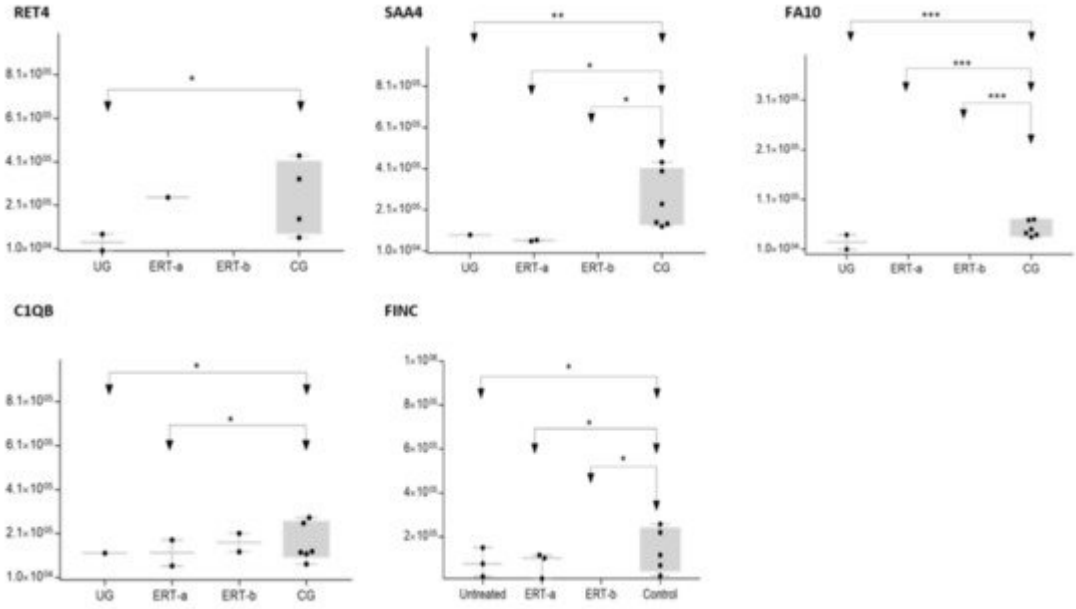

Figure 9. Box plot depicting expression levels of the 5 most relevant plasma proteins (RET4, SAA4, FA10, FINC, and C1QB) for which very low expression was observed in the UG and ERT-a and ERT-b groups relative to the control group (CG). Each data point represents the median value obtained in an individual sample. The line inside the box represents the median of all values obtained. The upper and lower limits of the box represent the first and third quartiles. Whiskers represent the minimum and maximum values within 1.5 times the interquartile range. Any data points not included between the whiskers are considered outliers. * $p < 0.05$; ** $p < 0.01$; *** $p < 0.001$.

The SWATH analysis identified proteins that were downregulated in the UG and the ERT-a and b groups relative to controls, or were absent entirely. These included FA10 and SAA4, which were absent in all patient groups, and RET4 and C1QB, which were absent in UG and in UG and ERT-a, respectively (see **Figure 9** and **Figure 10**).

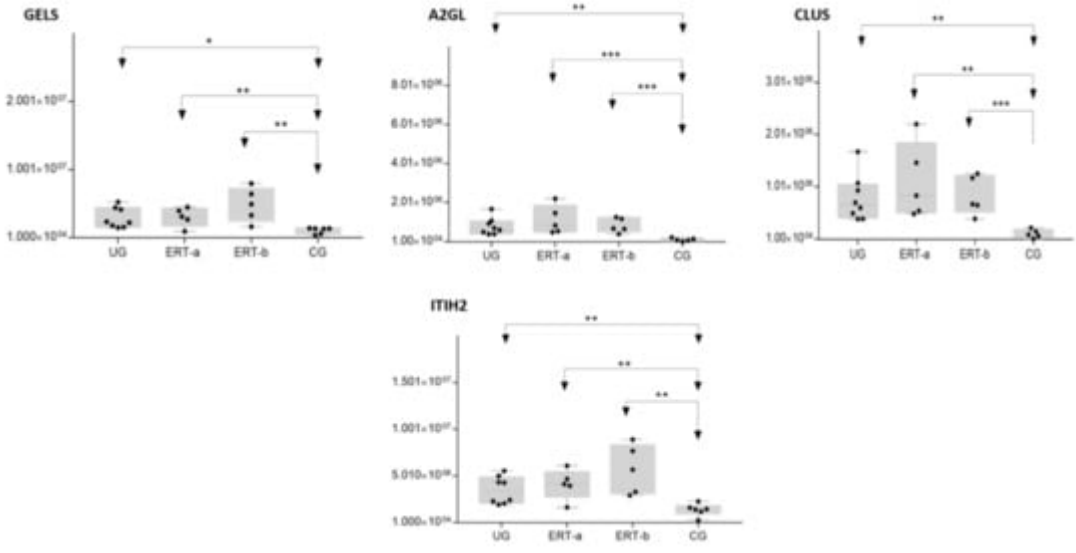

Figure 10. Box plot depictingthe4 plasma proteins (A2GL, CLUS, GELS, ITIH2) with the highest expression levels in the UG and ERT-a and ERT-b groups relative to the control group (CG). Each data point represents the median

value obtained in an individual sample. The line inside the box represents the median of all values obtained. The upper and lower limits of the box represent the first and third quartiles. Whiskers represent the minimum and maximum values within 1.5 times the interquartile range. Any data points not included between the whiskers are considered outliers. * $p < 0.05$; ** $p < 0.01$; *** $p < 0.001$.

In the UG group, we detected changes in expression in 4 proteins with respect to the 3 other groups (**Figure 11** and **Table 3**).

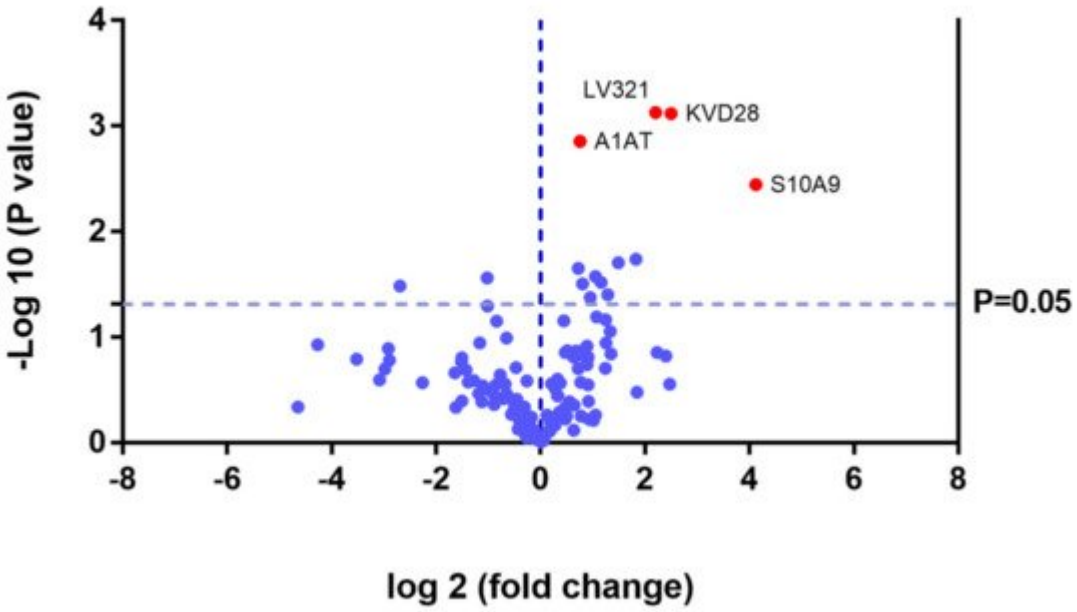

Figure 11. Volcano plot showing the results of the SWATH analysis of plasma protein expression. Data are represented as the results obtained for the untreated group (UG) relative to all other groups (CG, ERT-a, and ERT-b). Graph shows the negative base 10 log of the *p*-value plotted against the base 2 log of the fold change for each protein included in the SWATH analysis. Changes were considered significant at $p < 0.05$ and fold change >1.5.

Because these proteins were likely dysregulated as a consequence of the disease, they may include potential disease biomarkers that are either up-or down regulated in MPS IVA.

Theproteinsfor which changes in expression were detected in the UG included severalimmunoglobulins. This is unsurprising, given the important inflammatory component of MPS. Moreover, proteins that were dysregulated in this group included some previously proposed as biomarkers of MPS (e.g., A1AT[alpha 1 antitrypsin]) [32].We also observed dysregulation of proteins involved in inflammation (S10A9), binding to collagen (C1QC), and prothrombin (THRB), a thyroid hormone receptor that mediates the biological activities of thyroid hormone [33]. Proteins that were downregulated in the UG included C1QB (in line with previously reports, **Figure 8**) and the serine protease inhibitor A2AP (**Figure 9** and **Table 4**).

The most important dysregulated protein identified in this analysis was A1AT. Analysis of A1AT levels in individuals in each of the different groups (**Figure 12**) revealed significant upregulation in the UG compared with each of the

other groups. A1AT levels in the ERT-a and ERT-b groups were comparable to those observed in controls. This protein may constitute not only a biomarker of MPSIVA, but also an indicator of disease progression, potentially providing a better means of monitoring treatment responses in MPS IVA.

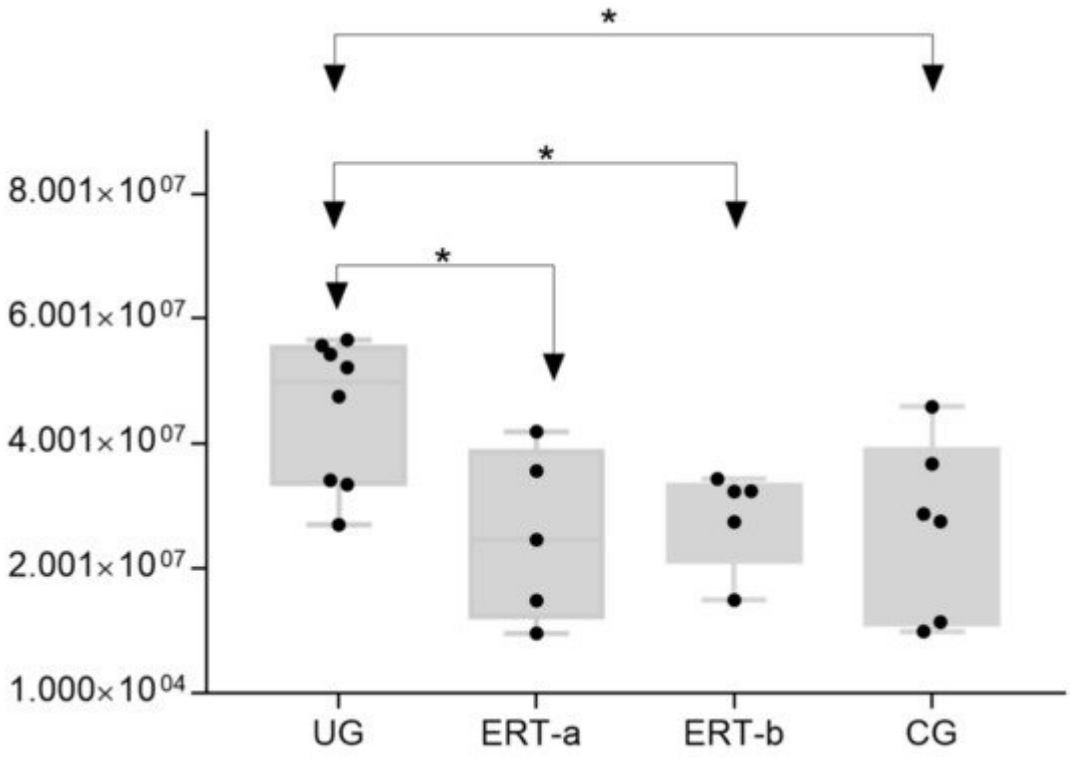

Figure 12. Box plot depicting ATA1 levels in each of the study groups. Each data point represents the median value obtained in an individual sample. The line inside the box represents the median of all values obtained. The upper and lower limits of the box represent the first and third quartiles. Whiskers represent the minimum and maximum values within 1.5 times the interquartile range. Any data points not included between the whiskers are considered outliers. * $p < 0.05$.

While treatment resulted in changes in the expression of proteins in both the ERT-a and ERT-b groups (**Table 4**), none of these proteins were common to both groups.

References

1. Matalon, R.; Arbogast, B.; Justice, P.; Brandt, I.K.; Dorfman, A. Morquio's syndrome: Deficiency of a chondroitin sulfate N-acetylhexosamine sulfate sulfatase. Biochem. Biophys Res. Commun. 1974, 61, 759–765.
2. Singh, J.; Di Ferrante, N.; Niebes, P.; Tavella, D. N-acetylgalactosamine-6-sulfate sulfatase in man. Absence of the enzyme in Morquio disease. J. Clin. Investig. 1976, 57, 1036–1040.

3. Di Ferrante, N.; Ginsberg, L.C.; Donnelly, P.V.; Di Ferrante, D.T.; Caskey, C.T. Deficiencies of glucosamine-6-sulfate or galactosamine-6-sulfate sulfatases are responsible for different mucopolysaccharidoses. Science 1978, 199, 79–81.
4. Tomatsu, S.; Yasuda, E.; Patel, P.; Ruhnke, K.; Shimada, T.; Mackenzie, W.G.; Mason, R.; Thacker, M.M.; Theroux, M.; Montaño, A.M.; et al. Morquio A syndrome: Diagnosis and current and future therapies. Pediatr. Endocrinol. Rev. PER 2014, 12 (Suppl. 1), 141–151.
5. Hendriksz, C.J.; Berger, K.I.; Giugliani, R.; Harmatz, P.; Kampmann, C.; Mackenzie, W.G.; Raiman, J.; Villarreal, M.S.; Savarirayan, R. International Guidelines for the Management and Treatment of Morquio A Syndrome. Am. J. Med. Genet. Part A 2015, 167, 11–25.
6. Khan, S.; Alméciga-Díaz, C.J.; Sawamoto, K.; Mackenzie, W.G.; Theroux, M.C.; Pizarro, C.; Mason, R.W.; Orii, T.; Tomatsu, S. Mucopolysaccharidosis IVA and glycosaminoglycans. Mol. Genet. Metab. 2017, 120, 78–95.
7. Peracha, H.; Sawamoto, K.; Averill, L.; Kecskemethy, H.; Theroux, M.; Thacker, M.; Nagao, K.; Pizarro, C.; Mackenzie, W.; Kobayashi, H.; et al. Diagnosis and prognosis of Mucopolysaccharidosis IVA. Mol. Genet. Metab. 2018, 125, 18–37.
8. Melbouci, M.; Mason, R.W.; Suzuki, Y.; Fukao, T.; Orii, T.; Tomatsu, S. Growth impairment in mucopolysaccharidoses. Mol. Genet. Metab. 2018, 124, 1–10.
9. Tomatsu, S.; Montaño, A.M.; Oikawa, H.; Smith, M.; Barrera, L.; Chinen, Y.; Thacker, M.M.; Mackenzie, W.G.; Suzuki, Y.; Orii, T. Mucopolysaccharidosis type IVA (Morquio A disease): Clinical review and current treatment. Curr. Pharm. Biotechnol. 2011, 12, 931–945.
10. Lavery, C.; Hendriksz, C. Mortality in patients with Morquio syndrome A. JIMD Rep. 2015, 15, 59.
11. Hendriksz, C.; Santra, S.; Jones, S.A.; Geberhiwot, T.; Jesaitis, L.; Long, B.; Qi, Y.; Hawley, S.M.; Decker, C. Safety, immunogenicity, and clinical outcomes in patients with Morquio A syndrome participating in 2 sequential open-label studies of elosulfasealfa enzyme replacement therapy (MOR-002/MOR-100), representing 5 years of treatment. Mol. Genet. Metab. 2018, 123, 479–487.
12. Hendriksz, C.J. Elosulfasealfa (BMN 110) for the treatment of mucopolysaccharidosis IVA (Morquio A Syndrome). Expert Rev. Clin. Pharmacol. 2016, 9, 1521–1532.
13. Akyol, M.U.; Alden, T.D.; Amartino, H.; Ashworth, J.; Belani, K.; Berger, K.I.; Borgo, A.; Braunlin, E.; Eto, Y.; Gold, J.I.; et al. Recommendations for the management of MPS IVA: Systematic evidence- and consensus-based guidance. Orphanet J. Rare Dis. 2019, 14, 137.
14. Tomatsu, S.; Sawamoto, K.; Shimada, T.; Bober, M.B.; Kubaski, F.; Yasuda, E.; Mason, R.W.; Khan, S.; Alméciga-Díaz, C.J.; Barrera, L.A.; et al. Enzyme replacement therapy for treating mucopolysaccharidosis type IVA (Morquio A syndrome): Effect and limitations. Expert Opin. Orphan Drugs 2015, 3, 1279–1290.

15. Tomatsu, S.; Montaño, A.M.; Dung, V.C.; Ohashi, A.; Oikawa, H.; Oguma, T.; Orii, T.; Barrera, L.; Sly, W.S. Enhancement of drug delivery: Enzyme-replacement therapy for murine Morquio A syndrome. Mol. Ther. 2010, 18, 1094–1102.
16. Sawamoto, K.; Stapleton, M.; Alméciga-Díaz, C.J.; Espejo-Mojica, A.J.; Losada, J.C.; Suarez, D.A.; Tomatsu, S. Therapeutic Options for Mucopolysaccharidoses: Current and Emerging Treatments. Drugs 2019, 79, 1103–1134.
17. Long, B.; Tompkins, T.; Decker, C.; Jesaitis, L.; Khan, S.; Slasor, P.; Harmatz, P.; O'Neill, C.A.; Schweighardt, B. Long-term Immunogenicity of Elosulfase Alfa in the Treatment of Morquio A Syndrome: Results From MOR-005, a Phase III Extension Study. Clin. Ther. 2017, 39, 118–129.
18. Doherty, C.; Stapleton, M.; Piechnik, M.; Mason, R.W.; Mackenzie, W.G.; Yamaguchi, S.; Kobayashi, H.; Suzuki, Y.; Tomatsu, S. Effect of enzyme replacement therapy on the growth of patients with Morquio A. J. Hum. Genet. 2019, 64, 625–635.
19. Tomatsu, S.; Averill, L.W.; Sawamoto, K.; Mackenzie, W.G.; Bober, M.B.; Pizarro, C.; Goff, C.J.; Xie, L.; Orii, T.; Theroux, M. Obstructive airway in Morquio A syndrome, the past, the present and the future. Mol. Genet. Metab. 2016, 117, 150–156.
20. Tomatsu, S.; Sawamoto, K.; Alméciga-Díaz, C.J.; Shimada, T.; Bober, M.B.; Chinen, Y.; Yabe, H.; Montaño, A.M.; Giugliani, R.; Kubaski, F.; et al. Impact of enzyme replacement therapy and hematopoietic stem cell transplantation in patients with Morquio A syndrome. Drug Des. Dev. Ther. 2015, 9, 1937–1953.
21. Qi, Y.; Musson, D.G.; Schweighardt, B.; Tompkins, T.; Jesaitis, L.; Shaywitz, A.J.; Yang, K.; O'Neill, C.A. Pharmacokinetic and Pharmacodynamic Evaluation of Elosulfase Alfa, an Enzyme Replacement Therapy in Patients with Morquio A Syndrome. Clin. Pharmacokinet. 2014, 53, 1137–1147.
22. De Franceschi, L.; Roseti, L.; Desando, G.; Facchini, A.; Grigolo, B. A molecular and histological characterization of cartilage from patients with Morquio syndrome. Osteoarthr. Cartil. 2007, 15, 1311–1317.
23. Fujitsuka, H.; Sawamoto, K.; Peracha, H.; Mason, R.W.; Mackenzie, W.; Kobayashi, H.; Yamaguchi, S.; Suzuki, Y.; Orii, K.; Orii, T.; et al. Biomarkers in patients with mucopolysaccharidosis type II and IV. Mol. Genet. Metab. Rep. 2019, 19, 100455.
24. Tan, H.T.; Chung, M.C.M. Label-Free Quantitative Phosphoproteomics Reveals Regulation of Vasodilator-Stimulated Phosphoprotein upon Stathmin-1 Silencing in a Pair of Isogenic Colorectal Cancer Cell Lines. Proteomics 2018, 18, e1700242.
25. Braccia, C.; Espinal, M.P.; Pini, M.; De Pietri Tonelli, D.; Armirotti, A. A new SWATH ion library for mouse adult hippocampal neural stem cells. Data Brief 2018, 18, 1–8.

26. Jayabalan, N.; Lai, A.; Nair, S.; Guanzon, D.; Scholz-Romero, K.; Palma, C.; McIntyre, H.D.; Lappas, M.; Salomon, C. Quantitative proteomics by SWATH-MS suggest an association between circulating exosomes and maternal metabolic changes in gestational diabetes mellitus. Proteomics 2019, 19, e1800164.
27. Jamwal, R.; Barlock, B.J.; Adusumalli, S.; Ogasawara, K.; Simons, B.L.; Akhlaghi, F. Multiplex and Label-Free Relative Quantification Approach for Studying Protein Abundance of Drug Metabolizing Enzymes in Human Liver Microsomes using SWATH-MS. J. Proteome Res. 2017, 16, 4134–4143.
28. Zhu, Y.; Zhu, J.; Lu, C.; Zhang, Q.; Xie, W.; Sun, P.; Dong, X.; Yue, L.; Sun, Y.; Yi, X.; et al. Identification of Protein Abundance Changes in Hepatocellular Carcinoma Tissues Using PCT–SWATH. Proteom. Clin. Appl. 2018, 1–13.
29. Li, H.; Mao, Y.; Xiong, Y.; Zhao, H.H.; Shen, F.; Gao, X.; Yang, P.; Liu, X.; Fu, D. A Comprehensive Proteome Analysis of Peripheral Blood Mononuclear Cells (PBMCs) to Identify Candidate Biomarkers of Pancreatic Cancer. Cancer Genom. Proteom. 2019, 16, 81–89.
30. Chang, R.Y.; Etheridge, N.; Nouwens, A.S.; Dodd, P.R. SWATH analysis of the synaptic proteome in Alzheimer’s disease. Neurochem. Int. 2015, 87, 1–12.
31. Gregorich, Z.R.; Ge, Y. Top-down proteomics in health and disease: Challenges and opportunities. Proteomics 2014, 14, 1195–1210.
32. Martell, L.; Lau, K.; Mei, M.; Burnett, V.; Decker, C.; Foehr, E.D. Biomarker analysis of Morquio syndrome: Identification of disease state and drug responsive markers. Orphanet J. Rare Dis. 2011, 6, 84.
33. Zhang, A.; Sieglaff, D.H.; York, J.P.; Suh, J.H.; Ayers, S.D.; Winnier, G.E.; Kharitonenkov, A.; Pin, C.; Zhang, P.; Webb, P.; et al. Thyroid hormone receptor regulates most genes independently of fibroblast growth factor 21 in liver. J. Endocrinol. 2015, 224, 289–301.